

# Experimental Study of EHD Conduction Pumping at the Micro-scale

Matthew R. Pearson and Jamal Seyed-Yagoobi

**Abstract**— Electrohydrodynamic (EHD) conduction pumping is now a well-researched phenomenon that can generate fluid flow in dielectric liquids. It offers many advantages over other EHD pumping methods, such as no degradation of the working fluid and no need for a temperature gradient. Studies to-date have focused on macro-scale devices with applied voltages on the order of 10 kV. However, like many other EHD concepts, conduction pumping generation depends primarily on the intensity of the imposed electric field. Therefore, at the micro-scale the reduced physical scale can be accompanied by a reduction in the magnitude of the applied voltage. The simplicity of EHD conduction pumps, such as the lack of moving parts, make it an attractive method for pressure generation in micro-scale fluid and heat transfer devices. This experimental study considers an EHD micro-pump formed by a rectangular mini-channel, 1 mm in height. Ten electrode pairs are arranged along the channel, flushed with the wall. The gap between the two electrodes of a pair is 250 microns, which is an order of magnitude less than previous studies. Static pressure head generation is measured along with power consumption. Pressure generation is achieved with considerably reduced applied voltage, and the ability of the pump to operate continuously over an extended period is also demonstrated.

**Index Terms**—Conduction Pumping, Electrohydrodynamics Microscale, Pressure Generation

## I. INTRODUCTION

ELECTROHYDRODYNAMIC (EHD) pumping methods rely on the interaction between electric fields and the flow fields of a dielectric fluid. The electric body force exerted on the fluid is [1]:

$$\mathbf{f}_e = \rho_e \mathbf{E} - \frac{1}{2} E^2 \nabla \epsilon + \frac{1}{2} \nabla \left[ E^2 \left( \frac{\partial \epsilon}{\partial \rho} \right)_T \rho \right] \quad (1)$$

The first term represents the Coulomb force that acts on free charges in an electric field. The second and third terms, titled dielectrophoretic and electrostriction forces respectively, represent the polarization force acting on polarized charges. The dielectrophoretic term requires a gradient in permittivity,

which is absent in an isothermal, single-phase fluid, while the electrostriction term is relevant only for compressible fluids.

Conduction pumping is a well-established EHD pumping mechanism that relies on the Coulomb force of Eq. (1). The net charge density,  $\rho_e$ , is established by field-enhanced dissociation of a neutral species into positive and negative ions. For a neutral species  $AB$  and its positive and negative ions,  $A^+$  and  $B^-$ , there is a reversible process of dissociation and recombination:



When the imposed electric field is low, the rates of dissociation and recombination are in dynamic equilibrium [2]. As the imposed electric field reaches a certain threshold, the rate of dissociation begins to increase (field-enhanced dissociation) while the rate of recombination remains approximately steady. Thus, beyond the electric double layer (EDL) that exists very close to the surface of the electrodes, there is another region called the heterocharge layer where the dissociation-recombination reactions are not in equilibrium. Due to the electric field, the charges redistribute so that there is a positive net charge density in the heterocharge layer surrounding the negative electrode, and vice versa for the positive electrode. The attraction of these charges to the adjacent electrode creates the Coulomb body force and can be used to generate a net flow when the electrode geometry is suitably designed. For further information about conduction pumping, including the fundamental governing equations and recent work in the field, see Ref. [3].

Many different electrode configurations have been studied. These can be broadly categorized into two groups: 1) penetrating electrodes and 2) flushed electrodes. In both cases, one electrode is flushed to the channel wall. For the penetrating electrode case, shown in Fig. 1a, the second electrode of each pair is inserted into channel. Early studies have considered hollow tube or needle electrodes inserted into the flow channel [2], [4], while later studies have achieved greater pressure generation by using perforated- or porous-plate electrodes [5] or multiple hollow tubes arranged side-by-side inside the channel [4], [6], [7]. A porous electrode design is shown schematically in Fig. 1a. There is a mostly radial attraction of the liquid to the flushed ring electrode and a mostly-axial attraction of the liquid to the flushed porous plate electrode. Therefore, the net force produced in the liquid is from left to right. In addition to the experimental studies considering simple pressure generation, EHD conduction pumps using penetrating electrodes have been successfully

Manuscript received April 17, 2009. This work was supported by the NASA Goddard Space Flight Center. Additional financial support was provided to the first author by the National Science Foundation Graduate Research Fellowship Program.

M. R. Pearson is with the Mechanical, Materials, and Aerospace Engineering Department, Illinois Institute of Technology, Chicago, IL 60616 USA (e-mail: pearmat@iit.edu).

J. Seyed-Yagoobi is with the Mechanical, Materials, and Aerospace Engineering Department, Illinois Institute of Technology, Chicago, IL 60616 USA (e-mail: yagoobi@iit.edu).

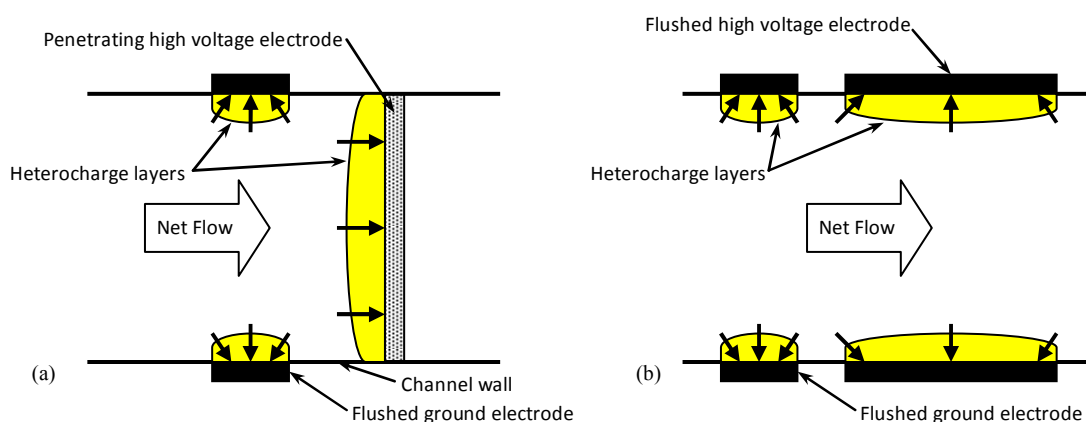


Fig. 1. Schematics showing a) penetrating-type electrodes and b) flushed-type electrodes. Heterocharge layers are shown along with arrows indicating the fluid attraction towards the electrodes.

used for flow generation in single-phase loops [8], two-phase loops [6], [7], heat pipes [9], and as an active flow-control device in a multiple-branch heat exchanger [10], [11]. Additionally, the study of EHD conduction-pumping-driven jets by Hanaoka et al. [12], [13] works on the same principle, but instead of the flow passing through a porous plate electrode, it is allowed to stagnate on a non-porous plate electrode.

Studies of flushed electrodes, where both electrodes are flush with the channel wall, are more limited. The clear advantage of using flushed electrodes is the minimization of drag on the flow; however, the body force introduced into the fluid is also reduced due to the nature of the body force distribution. If the electrodes are symmetric then there is an equal and opposite attraction to each electrode and the net force on the liquid is zero (assuming that positive and negative ions have equal charge mobility). However, if the electrodes are asymmetric, as shown in Fig. 1b, then there is a small net force from the narrow electrode to the wide electrode. This type of flushed electrode design was first presented by Siddiqui and Seyed-Yagoobi [14] to pump a liquid film (stratified two-phase flow) around a racetrack-style rectangular channel. In their case, electrodes were placed along the bottom wall of the channel only, as the upper boundary of the liquid was a free interface with the vapor phase. Compared to a penetrating electrode design that was also studied, the flushed electrode design performed better with thinner films (as low as 2 mm) by reducing the amount of drag on the flow.

Conduction pumping has a strong dependence on the imposed electric field. The characteristic electric field intensity is the voltage potential difference between the high-voltage and ground electrodes, divided by the spacing distance between them. Therefore, the distance between the two electrodes of an electrode pair is an important characteristic length often used in the non-dimensionalization of the governing equations. In all of the aforementioned studies, this characteristic length has been on the order of millimeters. Reducing this distance has important implications, as it allows

the same electric field intensity to be accomplished with lower applied voltages.

In the present study, EHD conduction pumping is used to pump a dielectric fluid through a mini-channel where the spacing distance between two electrodes of an electrode pair has been reduced to the micro-scale (by at least one order of magnitude from previous studies). Flushed electrodes are used to minimize the drag on the flow, since pressure losses from the channel become increasingly significant as the channel height is reduced.

## II. EXPERIMENTAL SETUP

The flow channel was formed by cutting circular disks from sheets of polytetrafluoroethane (PTFE) and type 316 stainless steel. The 1 mm x 15 mm flow channel cross-section and two additional holes for the electrical bus lines were then machined into each disk. Stainless steel disks formed the electrodes and PTFE disks formed the insulating spacers between electrodes. By selecting an appropriate thickness of the original sheet material, all electrode dimensions could be accurately controlled to within a tolerance of  $\pm 12.7 \mu\text{m}$ . The stainless steel disks were then polished and lightly etched to remove any sharp burrs and edges that might cause undesired ion-injection during operation. The resulting disks are shown in Fig. 2, and one electrode pair is seen assembled in Fig. 3. These disks were then stacked together inside a snug-fitting hollow cylinder of PTFE to form 10 electrode pairs, held together by the threaded bus lines and two stainless steel end caps.

This assembly, shown in Fig. 4, was placed inside a short length of stainless steel flanged pipe, held in place by four set screws in each end cap. One bus line (connecting the wide electrodes) was connected via a short length of PTFE-insulated cable to a power feed-through connector, and the other bus line was electrically connected to metallic pipe, which was electrically grounded. The metallic pipe provided a hermetic seal for the working fluid as well as an electrically-grounded shell protecting the user from any high voltage components. All disks were manufactured to high tolerances to ensure that the rectangular flow channel was aligned

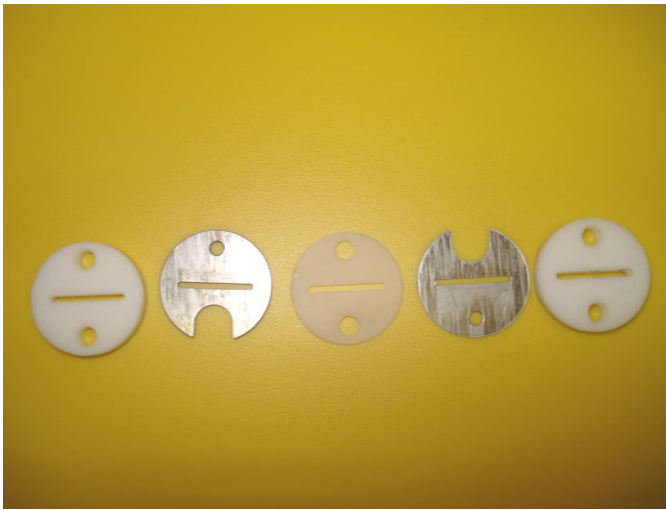


Fig. 2. The disks forming one electrode pair. From left-to-right: a thick PTFE spacer to separate the electrode pairs, a thin electrode disk, a thin PTFE spacer between electrodes of a single pair, a thick electrode disk, and a second thick PTFE spacer to separate the electrode pairs. The rectangular flow channel and the two holes/cut-outs for the electrical bus lines can be seen in each disk. The electrode disks contain a small hole for the bus line with which they must be in contact, and a larger cut-out for the bus line with which they must not be in contact.



Fig. 3. A photograph of one electrode pair, showing the end cap, the electrode assembly, and two threaded bus lines.



Fig. 4. The finished assembly, ready for insertion into the metal pipe.

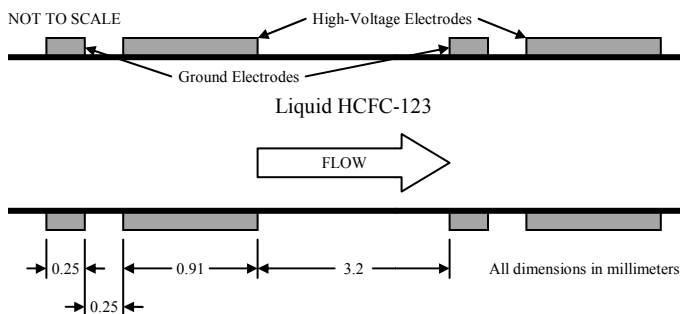
the pump that might reduce the pressure generation performance. The resulting electrode dimensions are shown in Fig. 5.

The working fluid was low-pressure refrigerant HCFC-123. Fluid purity becomes important as the spacing distance between electrodes is reduced because any conductive particles large enough to bridge this gap can cause a temporary or permanent short-circuit between the high voltage and ground electrodes, preventing further application of an electric field. The filling port of the apparatus was fitted with a Catch-All® C-032 refrigerant filter-drier by Sporlan, which has a nominal filter rating of 20 microns. All fluid entering the apparatus (either refrigerant or air) passed through this filter.

During assembly, all parts were soaked in and then rinsed with acetone. Once all parts were assembled and a pressure-tight seal was verified, a vacuum pump was connected to the drain port and the fill port was left open to the atmosphere. The vacuum pump was then operated for approximately 5 minutes, drawing air through the filter-drier and through the experiment and out through the drain port. The fill port was then connected to the refrigerant drum so that the vacuum pump could pull a deep vacuum inside the apparatus and the connecting hoses.

The drain port was then closed and the refrigerant drum valve was opened, drawing refrigerant into the apparatus. HCFC-123 is a good solvent so the refrigerant was allowed to rest overnight to dissolve any remaining residues inside the apparatus. This “dirty” refrigerant was then recovered to a deep vacuum and a fresh supply of refrigerant was delivered to the apparatus. This procedure was designed to maximize the purity of the working fluid, minimize the amount of particulates present, and avoid the trapping of air in the liquid phase portion of the system.

The pump, pressure transducer, and connecting lines were all completely filled with liquid refrigerant. Some vapor space was kept in a vertical branch pipe above the system to allow for thermal expansion due to small ambient temperature changes. As a result, the fluid in the pump was near saturation conditions. To avoid the formation of vapor bubbles in the pumping system, either due to heat added by Joule heating of the fluid by the applied electric field or due to minor changes in ambient temperature, compressed air was added to the vapor space to bring the system pressure to about 150 kPa absolute (compared to the HCFC-123 saturation pressure of



76 kPa absolute at 20°C).

Fig. 5. Electrode dimensions in millimeters.

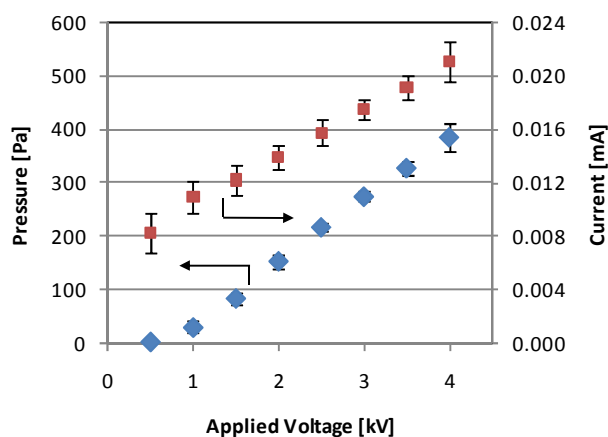


Fig. 7. Pressure generation and current as a function of applied voltage.

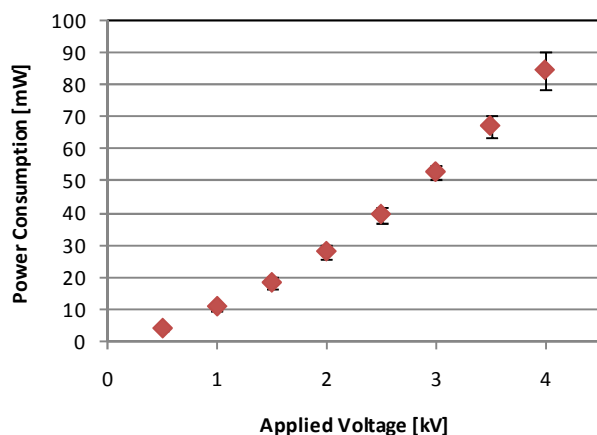


Fig. 8. Power consumption as a function of applied voltage

To minimize any in-situ degradation of the fluid due to material corrosion, the primary wetted materials were 316 stainless steel and PTFE. The only exceptions were small components, particularly the power feed-through and sight glass, that had small amounts of the following as wetted materials: soda-lime glass, alumina ceramic, nickel, 18-8 stainless steel, and beryllium copper.

The voltage was applied to the high-voltage electrodes by a Glassman High Voltage power supply, model EH30R3. Pressure was measured by a Validyne DP15 differential pressure transducer with diaphragm no. 3-022 (maximum differential pressure of 1.4 kPa). The pressure transducer was calibrated using a water-filled U-tube manometer. Once fitted in the apparatus, the pressure transducer was protected from over-pressurization by a bypass valve that was opened during vacuuming, cleaning, and filling operations and closed during data acquisition.

The experimental uncertainty in the pressure reading was below 1%. The uncertainty in the current was 20% for the minimum measured current of 8  $\mu$ A, reducing to less than 10% at current values exceeding 17  $\mu$ A. The uncertainty in the power consumption was less than 25% for all cases of 2 kV or higher applied voltages.

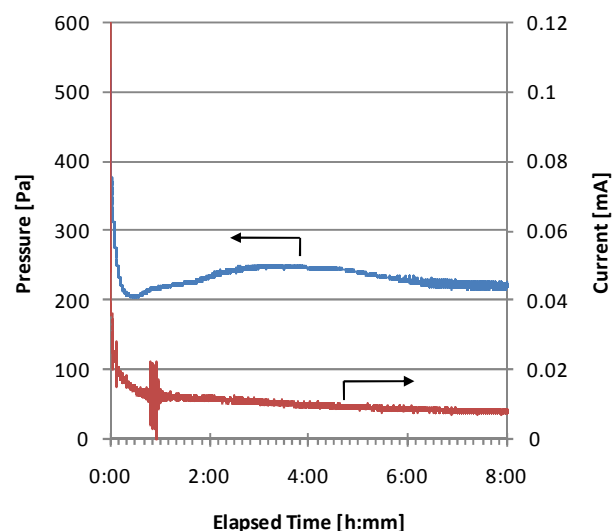


Fig. 6. Timeline showing pressure generation and power consumption during an 8-hour running duration with 2 kV applied voltage.

### III. EXPERIMENTAL RESULTS AND DISCUSSION

To study the pressure generation at a variety of applied voltages, a step-voltage profile was applied to the pump in 0.5 kV increments from 0 kV to 4 kV. Each voltage was held for five minutes to allow the pressure and current to reach steady state. The current and pressure signals were sampled at 100 Hz and data from the last 60 seconds of each applied voltage interval were then averaged to provide a data point at that voltage. The complete procedure was repeated six times to provide the standard deviation bars shown in the figures.

Figure 7 shows the pressure generation and current as a function of applied voltage. Figure 8 shows the corresponding power consumption. Pressure increased continuously with applied voltage to a value of around 390 Pa at 4 kV. The corresponding power consumption at this applied voltage was approximately 85 mW. At voltages of 3 kV or less, the pressure and current values were relatively steady. At higher voltages, there were large time-varying fluctuations that were likely caused by the fluid being close to dielectric breakdown.

In order to study the long-term performance of the pump, an extended duration test was also conducted in which a 2 kV applied voltage was sustained for a period of 8 hours. The pressure generation and current of the EHD pump over this duration are shown as a timeline in Fig. 6. Upon initial application of the electric field, pressure and current levels spiked near 300 Pa and 140  $\mu$ A, respectively, before quickly decaying to much lower values of about 200 Pa and less than 20  $\mu$ A. This decay behavior is commonplace when dielectric fluids are suddenly subject to a strong dc electric field. Note that after about 50 minutes of operation, wide oscillations in current occurred over a span of about 10 minutes. These oscillations were likely caused by a stray particle becoming caught in the pumping section. If that particle is electrically conductive, then it can briefly change the local fluid conductivity or cause electrical breakdown of the electric field

due to local electric field intensification and ion-injection. Since this study considered static pressure generation, there was no net flow through the pumping section. Therefore, particles could remain trapped in the pumping section for a long time whereas in the presence of net flow, they would likely pass through the pumping section quickly. Throughout the remainder of the 8-hour period, the current consumption continued to gradually decay, reaching about 9  $\mu\text{A}$  by the end of the eight hour test period. The measured pressure generation after the initial decay period remained in the range of 200–250 Pa.

It must be noted that the pressure generation at 2 kV for the step-increasing voltage study (Fig. 7) is approximately 50 kPa lower than the minimum pressure reading during the eight-hour test at the same applied voltage (Fig. 6). This appears to be due to a hysteresis effect, – both pressure generation and power consumption both exhibit some variation based on the manner in which the voltages have been applied over a recent history.

#### IV. CONCLUSIONS

The results successfully demonstrate EHD conduction pumping with micro-scale, flushed electrodes in a thin, rectangular channel. The reduced dimensions allow operation at much lower voltages, and the flushed electrodes impose a negligible amount of drag on the fluid compared to penetrating electrode designs. Note that an EHD conduction pump with multiple electrode pairs is really a multi-stage pump, with each electrode pair acting as one stage. Therefore, pressure head generation can be further increased simply by increasing the number of electrode pairs. Power consumption remained very low – less than 90 mW even at the maximum applied voltage. The success of this study suggests that, with improved fluid filtration, the electrode dimensions and channel height can be further reduced with the ultimate objective of pumping in a micro-channel with voltage levels below 1 kV.

#### REFERENCES

- [1] J. R. Melcher, *Continuum Electromechanics*. Cambridge, MA: MIT Press, 1981.
- [2] P. Atten and J. Seyed-Yagoobi, "Electrohydrodynamically induced dielectric liquid flow through pure conduction in point/plane geometry," *IEEE Transactions on Dielectrics and Electrical Insulation*, vol. 10, no. 1, pp. 27–36, 2003.
- [3] M. R. Pearson and J. Seyed-Yagoobi, "Advances in electrohydrodynamic conduction pumping," *IEEE Transactions on Dielectrics and Electrical Insulation*, vol. 16, no. 2, pp. 424–434, Apr. 2009.
- [4] S.-I. Jeong and J. Seyed-Yagoobi, "Experimental study of electrohydrodynamic pumping through conduction phenomenon," *Journal of Electrostatics*, vol. 56, no. 2, pp. 123–133, 2002.
- [5] S.-I. Jeong and J. Seyed-Yagoobi, "Innovative electrode designs for electrohydrodynamic conduction pumping," *IEEE Transactions on Industry Applications*, vol. 40, no. 3, pp. 900–904, May 2004.
- [6] S.-I. Jeong and J. Didion, "Thermal control utilizing an electrohydrodynamic conduction pump in a two-phase loop with high heat flux source," *Journal of Heat Transfer*, vol. 129, no. 11, pp. 1576–1583, 2007.
- [7] S.-I. Jeong and J. Didion, "Performance characteristics of electrohydrodynamic conduction pump in two-phase loops," *Journal of Thermophysics and Heat Transfer*, vol. 22, no. 1, pp. 90–97, 2008.
- [8] Y. Feng and J. Seyed-Yagoobi, "Understanding of electrohydrodynamic conduction pumping phenomenon," *Physics of Fluids*, vol. 16, no. 7, pp. 2432–2441, 2004.
- [9] S.-I. Jeong and J. Seyed-Yagoobi, "Performance enhancement of a monogroove heat pipe with electrohydrodynamic conduction pumping," in *Proceedings of the ASME International Mechanical Engineering Congress and Exposition*, New Orleans, LA, 2002.
- [10] Y. Feng and J. Seyed-Yagoobi, "Control of liquid flow distribution utilizing EHD conduction pumping mechanism," *IEEE Transactions on Industry Applications*, vol. 42, no. 2, pp. 369–377, 2006.
- [11] Y. Feng and J. Seyed-Yagoobi, "Control of adiabatic two-phase dielectric fluid flow distribution with EHD conduction pumping," *Journal of Electrostatics*, vol. 64, no. 7–9, pp. 621–627, 2006.
- [12] R. Hanaoka, S. Takata, M. Murakumo, and H. Anzai, "Properties of liquid jet induced by electrohydrodynamic pumping in dielectric liquids," *Electrical Engineering in Japan*, vol. 138, no. 4, pp. 1–9, 2002, [Denki Gakkai Ronbunshi, vol. 121-A, no. 3, pp. 224–230, March 2001].
- [13] R. Hanaoka, H. Nakamichi, S. Takata, and T. Fukami, "Distinctive flow properties of liquid jet generated by EHD pump and conical nozzle," *Electrical Engineering in Japan*, vol. 154, no. 1, pp. 9–19, 2006, [Denki Gakkai Ronbunshi, vol. 124-A, no. 5, pp. 399–406, May 2004].
- [14] M. A. Siddiqui and J. Seyed-Yagoobi, "Experimental study of pumping of liquid film with electric conduction phenomenon," *IEEE Transactions on Industry Applications*, submitted for publication.